Relativistic nuclear matter in generalized thermo-statistics

K. Miyazaki

E-mail: miyazakiro@rio.odn.ne.jp

Abstract

The generalized Fermi-Dirac thermo-statistics is developed for relativistic nuclear matter. We introduce the generalized thermodynamic potential using the q-deformed exponential and logarithm. The baryon density has a form of the q-expectation value. Then, we use the mapping of the non-extensive thermo-statistics onto the extensive one. Therefore, the Clausius extensive entropy and the physical intensive temperature are determined through the Gibbs thermodynamic relation. The power-law index is constrained into a region $1 < q < 4/3$ and assumed to be density dependent. The pressure-density isotherms exhibit the liquid-gas phase transition. The calculated critical temperature agrees with the experimental value for finite nuclei of intermediate masses. There is little difference in the boiling temperatures from the standard and generalized thermo-statistics, although the latter improves the caloric curve of nuclear liquid. It is found that the cut-off prescription by Teweldeberhan *et al.* for the generalized Fermi-Dirac distribution breaks the third-law of thermodynamics.

1 Introduction

Now, the thermo-statistics generalized by power-law [1,2] has been acknowledged to be beyond the standard Boltzmann-Gibbs thermo-statistics and applicable to non-equilibrium systems, small systems, gravitational systems and others. (The comprehensive references are found in Ref. [3].) Although the theoretical origin [4] of the power-law is still an open problem, the generalized thermo-statistics is also useful [5-7] in nuclear physics.

In the present paper we investigate warm nuclear matter in the relativistic mean-field (RMF) model [8] within the generalized thermo-statistics. Although there have been already similar works [9,10], our investigation is essentially different from them in the following respects. 1) We use the RMF model of field-dependent meson-nucleon coupling constants developed in Ref. [11]. The field-dependence is due to many-body correlation in dense nuclear medium. The correlation might lead to the power-law. 2) The baryon densities in Refs. [9,10] do not have the forms of q-expectation but the normal ones. 3) We introduce the physical intensive temperature and the conjugate extensive entropy [12-14] through the Gibbs thermodynamic relation.

2 Generalized Fermi-Dirac thermo-statistics

In the standard Fermi-Dirac thermo-statistics[1], the thermodynamic potential per volume of nuclear matter in the RMF model [8] is

$$\Omega = \frac{1}{2} m_\sigma^2 \langle\sigma\rangle^2 - \frac{1}{2} m_\omega^2 \langle\omega_0\rangle^2 - \gamma\, k_B T \int \frac{d^3\mathbf{k}}{(2\pi)^3} \ln\left[1 + \exp\left(\frac{\nu - E^*(k)}{k_B T}\right)\right]. \tag{1}$$

We have neglected the effect of anti-nucleon. M^* and $E^*(k) = (\mathbf{k}^2 + M^{*2})^{1/2}$ are the effective mass and the energy of nucleon in nuclear matter. The Boltzmann constant is k_B. The spin-isospin degeneracy is $\gamma = 4$. The ν is defined using the chemical potential μ and the vector potential V of nucleon as

$$\nu = \mu - V. \tag{2}$$

Then, in order to develop the generalized Fermi-Dirac thermo-statistics, we extend Eq. (1) by replacing $\exp(x)$ and $\ln(x)$ with q-deformed functions:

$$\exp_q(x) \equiv [\,1 + (1-q)\,x\,]^{1/(1-q)}\,, \tag{3}$$

$$\ln_q(x) \equiv \frac{x^{1-q} - 1}{1-q}. \tag{4}$$

Therefore, we have

$$\Omega_q = \frac{1}{2} m_\sigma^2 \langle\sigma\rangle^2 - \frac{1}{2} m_\omega^2 \langle\omega_0\rangle^2 - \gamma\, k_B T_q \int \frac{d^3\mathbf{k}}{(2\pi)^3} \frac{(Z_q(k))^{1-q} - 1}{1-q}, \tag{5}$$

where

$$Z_q(k) = 1 + \left[1 + (1-q)\,\frac{\nu - E^*(k)}{k_B T_q}\right]^{\frac{1}{1-q}}. \tag{6}$$

A suffix q has been attached to temperature because as shown below T_q is not a physical intensive temperature. Consequently, the baryon density is

$$\rho_B = -\frac{\partial\,\Omega_q}{\partial\mu} = \gamma\, k_B T_q \int \frac{d^3\mathbf{k}}{(2\pi)^3} \frac{1}{(Z_q(k))^q} \frac{\partial Z_q}{\partial\mu} = \gamma \int \frac{d^3\mathbf{k}}{(2\pi)^3} (n_q(k))^q, \tag{7}$$

where the generalized Fermi-Dirac distribution is

$$n_q(k) = (Z_q(k))^{-1} \left[1 + (1-q)\,\frac{\nu - E^*(k)}{k_B T_q}\right]^{\frac{1}{1-q}} = \frac{1}{1 + \left[1 + (q-1)\,\frac{E^*(k) - \nu}{k_B T_q}\right]^{\frac{1}{q-1}}}. \tag{8}$$

Although the precise derivation of the generalized Fermi-Dirac distribution has been

[1] In the present paper the Fermi-Dirac thermo-statistics means the thermodynamics based on the quantum statistical mechanics of relativistic spin-1/2 particle.

attempted in Ref. [15], Eq. (8) is widely acknowledged [9,10,16,17] to be useful. The baryon density (7), which has a form of q-expectation, is the same as Ref. [17] but is different from Refs. [9,10] where the normal expectations are used.

As will be shown in Appendix we can derive the entropy in differentiating Ω_q by T_q. In the present work we however introduce the extensive entropy S through the Gibbs thermodynamic relation [13]:

$$\Omega_q = U_q - TS - \mu\,\rho_B. \tag{9}$$

(Precisely, S is the entropy per volume and S/ρ_B is the entropy per baryon. Both the quantities can be defined only for extensive entropy but not for non-extensive one.) U_q is the energy density defined by

$$U_q = \gamma \int \frac{d^3\mathbf{k}}{(2\pi)^3} \left(E^*(k) + V\right) \left(n_q(k)\right)^q + \frac{1}{2} m_\sigma^2 \langle\sigma\rangle^2 - \frac{1}{2} m_\omega^2 \langle\omega_0\rangle^2 . \tag{10}$$

The intensive quantity T, which is conjugate to the extensive entropy S, is just the physically observed temperature. To the contrary T_q is only an inverse of the Lagrange multiplier [17]. In this sense our theory is the *extensive thermo-statistics* generalized by power-law. Here, it is noted [1] that the power-law is also involved in the non-extensive thermo-statistics. If the power-law index is identical to the non-extensivity index, we can utilize the mapping [13,14,18] of the non-extensive thermo-statistics onto the extensive one. Both of the intensive temperature T and the extensive entropy S are derived from the proper non-extensive entropy $\bar{S}_q$ [1]:

$$\bar{S}_q(A \oplus B) = \bar{S}_q(A) + \bar{S}_q(B) + (1-q)\,\bar{S}_q(A)\,\bar{S}_q(B). \tag{11}$$

In practice the non-extensivity (11) is equivalent to the extensivity,

$$\ln\left[1 + (1-q)\,\bar{S}_q(A \oplus B)\right] = \ln\left[1 + (1-q)\,\bar{S}_q(A)\right] + \ln\left[1 + (1-q)\,\bar{S}_q(B)\right]. \tag{12}$$

We can therefore define [12,13] the Clausius extensive entropy, which satisfies the first law of thermodynamics:

$$\frac{S}{\rho_B} = \frac{\ln C_q}{1-q}, \tag{13}$$

where

$$C_q = 1 + (1-q)\,\bar{S}_q. \tag{14}$$

The conjugate intensive temperature [12-14] is given by

$$T = C_q\,T_q. \tag{15}$$

The explicit expression of $\bar{S}_q$ is not necessary because it is calculated through the Gibbs thermodynamic relation (9). For a definite value of physical temperature T, given a trial value of $\bar{S}_q$, the virtual temperature T_q is determined from Eq. (15). Once T_q is given, the thermodynamic potential, the energy density and the baryon density are calculated. Then, the extensive entropy S is calculated from the Gibbs thermodynamic relation (9). Finally, the non-extensive entropy $\bar{S}_q$ is calculated again from Eq. (13). The procedure is iterated until the value of $\bar{S}_q$ is converged. On the other hand, for a definite value of virtual temperature T_q, the thermodynamic relation becomes a nonlinear equation to determine physical temperature T:

$$\frac{T\,\ln\left(T/T_q\right)}{1-q} = \frac{U_q - \Omega_q}{\rho_B} - \mu. \tag{16}$$

The effective mass M^* and the vector potential V are determined by extremizing the thermodynamic potential Ω_q. The resultant equations are formally the same as those at $T = 0$:

$$\begin{aligned}\frac{\partial\,\Omega_q}{\partial\,M^*} = \rho_S - (1-m^*)\left[1 + (1-\lambda)\,\frac{(1-m^*)\,m^*}{h}\right]\left(\frac{m_\sigma}{g^*_{NN\sigma}}\right)^2 M & \\ + (1-\lambda)\,\frac{m^* v^2}{h}\left(\frac{m_\omega}{g^*_{NN\omega}}\right)^2 M &= 0,\end{aligned} \tag{17}$$

$$\begin{aligned}\frac{\partial\,\Omega_q}{\partial\,V} = \rho_B - \left[1 + (1-\lambda)\,\frac{v^2}{h}\right] v\left(\frac{m_\omega}{g^*_{NN\omega}}\right)^2 M & \\ + (1-\lambda)\,\frac{(1-m^*)^2\,v}{h}\left(\frac{m_\sigma}{g^*_{NN\sigma}}\right)^2 M &= 0,\end{aligned} \tag{18}$$

where M is the free nucleon mass, $M^* = m^* M$ and $V = v\,M$. The scalar density is defined as

$$\rho_S = \gamma \int \frac{d^3\mathbf{k}}{(2\pi)^3}\frac{M^*}{E^*(k)}\left(n_q(k)\right)^q. \tag{19}$$

The effective meson-nucleon coupling constant is given by [11]

$$g^*_{NN\sigma(\omega)} = h\,g_{NN\sigma(\omega)} = \frac{1}{2}\left[(1+\lambda) + (1-\lambda)\left(m^{*2} - v^2\right)\right] g_{NN\sigma(\omega)}. \tag{20}$$

The free meson-nucleon coupling constants $g_{NN\sigma}$ and $g_{NN\omega}$ and the renormalization parameter λ are determined so as to reproduce the properties of nuclear matter at saturation. Their values are found in Table 1 of Ref. [11].

3 Numerical analyses

We have already investigated in Ref. [19] the standard Fermi-Dirac thermo-statistics of nuclear matter and found the critical temperature $T = 16.47$MeV. (Although the effect of anti-nucleon is taken into account in Ref. [19], it is negligible below $T = 20$MeV.) The value agrees well with the empirical one [20] $T = 16.6 \pm 0.86$MeV. There is therefore no room to introduce the generalized thermo-statistics. However, the above value is for infinite nuclear matter. The critical temperatures for finite nuclei [21] are lower than it. The present paper studies whether the properties of warm finite nuclei are reproduced in the generalized thermo-statistics of nuclear matter.

Using a partial integration in Eq. (5) we have

$$-\,\Omega_q = P + \frac{\gamma\, k_B T}{6\,\pi^2}\left(\frac{q-1}{k_B T}\right)^{\frac{1}{1-q}} k^{\frac{4-3q}{1-q}}\Big|_{k\to\infty}, \tag{21}$$

where P is the pressure,

$$P = \frac{\gamma}{3}\int \frac{d^3\mathbf{k}}{(2\pi)^3}\frac{k^2}{E^*(k)}\left(n_q(k)\right)^q - \frac{1}{2}\,m_\sigma^2\,\langle\sigma\rangle^2 + \frac{1}{2}\,m_\omega^2\,\langle\omega_0\rangle^2\,. \tag{22}$$

The thermodynamic relation $P = -\,\Omega_q$ therefore requires

$$1 < q < 4/3. \tag{23}$$

This constraint is also imposed on the first term in Eq. (22). In fact, following to the similar analysis in Ref. [10], the first term behaves asymptotically in the limit $k \to \infty$:

$$\int \frac{d^3\mathbf{k}}{(2\pi)^3}\frac{k^2}{E^*(k)}\left(n_q(k)\right)^q \;\to\; \frac{k^4}{k^{\frac{q}{q-1}}} = k^{\frac{4-3q}{1-q}}. \tag{24}$$

The asymptotic behavior of the first term in the energy density (10) is also the same. The pressure and the energy density are finite only if the power-law index satisfies the condition (23). Moreover, the baryon density (7) behaves asymptotically as

$$\int \frac{d^3\mathbf{k}}{(2\pi)^3}\left(n_q(k)\right)^q \;\to\; \frac{k^3}{k^{\frac{q}{q-1}}} = k^{\frac{3-2q}{1-q}}, \tag{25}$$

and so a constraint $1 < q < 3/2$ is imposed, while the scalar density (19) behaves asymptotically as

$$\int \frac{d^3\mathbf{k}}{(2\pi)^3}\frac{M^*}{E^*(k)}\left(n_q(k)\right)^q \;\to\; \frac{k^2}{k^{\frac{q}{q-1}}} = k^{\frac{2-q}{1-q}}, \tag{26}$$

and so a constraint $1 < q < 2$ is imposed. In general the second law of thermodynamics [22] also requires $q < 2$. Consequently, Eq. (23) is the condition for finite values of the pressure, the energy density, the baryon and scalar densities. It is looser than the condition $1 < q < 5/4$ in Ref. [10] because of the q-expectations in Eqs. (22) and (24)-(26) against the normal expectations in Ref. [10].

We have introduced the physical intensive temperature in Eq. (15). It may be however negative for $q > 1$ because the entropy is generally large at low density. (See Eq. (13).) So as to avoid a problem $|q - 1| \ll 1$ should be satisfied at low baryon densities. In the present work we assume that the power-law index depends on the baryon density as follows:

$$q - 1 = \frac{1}{3} \frac{\rho_B/\rho_0}{\rho_B/\rho_0 + 2}, \tag{27}$$

where ρ_0 is the saturation density. At present the physical origin of power-law is an open problem. If it is due to the many-body correlation incorporated in the effective coupling constant (20), the density dependence of power-law index is reasonable because the correlation is stronger at higher density.

We still have to specify the cut-off prescription [17] for the generalized Fermi-Dirac distribution (8), which can be defined precisely only for $1 + (q-1)\frac{E^*(k)-\nu}{k_B T_q} > 0$. Here, we follow the standard Tsallis prescription:

$$n_q(k) = \begin{cases} \dfrac{1}{1 + \left[1 + (q-1)\frac{E^*(k)-\nu}{k_B T_q}\right]^{\frac{1}{q-1}}} & \text{for} \quad 1 + (q-1)\dfrac{E^*(k)-\nu}{k_B T_q} > 0 \\ 1 & \text{for} \quad 1 + (q-1)\dfrac{E^*(k)-\nu}{k_B T_q} \leq 0 \end{cases}. \tag{28}$$

For definite physical temperature T and the baryon density ρ_B we solve 4th-rank non-linear simultaneous equations (7), (9), (17) and (18) using Newton-Raphson algorithm, so that we have the effective mass M^*, the vector potential V, the chemical potential μ and the non-extensive entropy $\bar{S}_q$. The pressure, the energy density and the extensive entropy are determined at a time. Figure 1 shows the isotherms on pressure-density plane. (In the following calculations we set $k_B = 1$.) They exhibit typical nature of van der Waals equation-of-state. The critical temperature is $T = 12.09$MeV and the critical point lies on $P = 0.2296\text{MeV/fm}^3$ and $\rho_B = 0.058\text{fm}^{-3}$. The flash temperature, above which the pressure is always positive at any density, is $T = 10.46$MeV. Both the temperatures are lower than the values [19] in the standard Fermi-Dirac thermo-statistics. However, the critical temperature agrees with $T = 12.4 \pm 0.99$MeV [21] for finite nuclei of $140 < A < 180$. The result suggests that the generalized thermo-statistics of nuclear matter takes into account finiteness of nuclei.

The black and red curves in Fig. 2 show the pressure-density isotherms at $T = 10$MeV in the standard and generalized thermo-statistics, respectively. There is large difference between the dotted parts in the two curves, which correspond to the liquid-gas phase transition. Because we are founded on the extensive entropy in Eq.

(9), the phase equilibrium condition is the same as the standard Gibbs one. Therefore, the Maxwell construction of phase equilibrium between liquid and gas phases leads to the horizontal lines, while the dotted parts are not physically realized. We see that in the equilibrium pressure of liquid-gas mixed phase there is little difference between the standard and generalized thermo-statistics.

Next, at definite pressure $P = 0.01\mathrm{MeV/fm}^3$ we calculate the caloric curve by solving 4th-rank nonlinear simultaneous equations (7), (17), (18) and (22), so that we have the effective mass M^*, the vector potential V, the chemical potential μ and the virtual temperature T_q. The physical temperature T is determined from Eq. (16). Then, the extensive entropy is calculated from Eq. (13). The result is shown by the red curve in Fig. 3 while the black curve is the result in the standard Fermi-Dirac thermo-statistics. The horizontal lines are the boiling temperatures from the Maxwell construction of liquid-gas phase equilibrium. The experimental data are from Ref. [23]. Although there is little difference in the two boiling temperatures, the generalized thermo-statistics improves the caloric curve in the region of low excitation or nuclear liquid.

We have used the cut-off prescription (28) for the generalized Fermi-Dirac distribution, while Ref. [10] used another one proposed in Ref. [17]:

$$n_q(k) = \begin{cases} \dfrac{1}{1+\left[1+(q-1)\frac{E^*(k)-\nu}{k_B T_q}\right]^{\frac{1}{q-1}}} & \text{for} \quad E^*(k)-\nu > 0 \\ \dfrac{1}{1+\left[1+(1-q)\frac{E^*(k)-\nu}{k_B T_q}\right]^{\frac{1}{1-q}}} & \text{for} \quad E^*(k)-\nu \le 0 \end{cases}. \tag{29}$$

This is based on a requirement that the q-deformed exponential satisfies the similar relation $\exp_q(-x) = 1/\exp_q(x)$ to $\exp(-x) = 1/\exp(x)$ of the normal exponential. We have recalculated the caloric curve using (29) but found that the third-law of thermodynamics is broken. As a matter of fact Fig. 4 shows the Clausius entropy per baryon S/ρ_B as a function of the physical temperature T. The solid and dotted curves are the results using the cut-off prescription (28) and (29), respectively. The dashed curve is the result in the standard Fermi-Dirac thermo-statistics. We really see $\lim_{T\to 0}(S/\rho_B) = 0$ for Eq. (28) but $S/\rho_B = 0$ at $T > 0$ for Eq. (29). The problem caused by Eq. (29) might be characteristic of our model of the generalized thermo-statistics. It is however concluded that the standard Tsallis prescription (28) is robust in application of the generalized Fermi-Dirac distribution.

4 Summary

We have investigated the generalized thermo-statistics of nuclear matter. Our formulation starts at the q-deformed thermodynamic potential expressed in terms of the q-deformed exponential and logarithm. The baryon density is directly obtained in differentiating the thermodynamic potential by chemical potential. It has a form of the q-expectation value. We have used the mapping of the non-extensive thermo-statistics onto the extensive one, so that the Clausius extensive entropy and the conjugate intensive temperature are determined through the Gibbs thermodynamic relation.

The power-law index is constrained into a region $1 < q < 4/3$ so as to produce finite values of pressure, energy density, baryon and scalar densities. Moreover, the index is assumed to be density dependent so that the physical intensive temperature is not negative at low baryon densities. We have calculated the pressure-density isotherms. They exhibit the nature of van der Waals equation-of-state. The calculated critical temperature is lower than the empirical value for infinite nuclear matter but agrees with the experimental value for finite nuclei of intermediate masses. The generalized thermo-statistics can take into account the effect by finiteness of nuclei. In the equilibrium pressure of liquid-gas mixed phase from the Maxwell construction, there is little difference between the standard and generalized thermo-statistics.

Next, we have calculated the caloric curve. In the boiling temperature from the Maxwell construction of liquid-gas mixed phase there is also little difference between the standard and generalized thermo-statistics. However, the latter improves the caloric curve in pure phase of nuclear liquid. Moreover, we have investigated the two cut-off prescriptions by Tsallis and by Teweldeberhan *et al.* for the generalized Fermi-Dirac distribution. It is found that the latter breaks the third-law of thermodynamics.

In the present paper we have considered symmetric nuclear matter. In practice the nuclear liquid-gas phase transition is experimentally investigated in heavy-ion reactions, which produce the asymmetric nuclear matter. It is the binary system that has two independent chemical potentials of proton and neutron. The phase transition in binary system cannot be described in the Maxwell construction, but we need the Gibbs construction [24] to take into account the equilibrium of two chemical potentials. In a future work we will extend the present investigation to asymmetric nuclear matter.

Appendix

Here, we derive the entropy from differentiating the thermodynamic potential (5) by virtual temperature. Because Eq. (6) is rewritten as

$$\frac{\nu - E^*(k)}{k_B T_q} = \frac{\left(Z_q(k) - 1\right)^{1-q} - 1}{1-q}, \tag{30}$$

we have

$$S_q = -\frac{\partial \Omega_q}{\partial T_q} = \gamma\, k_B \int \frac{d^3\mathbf{k}}{(2\pi)^3} \left[\frac{\left(Z_q(k)\right)^{1-q} - 1}{1-q} - \left(n_q(k)\right)^q \frac{\left(Z_q(k) - 1\right)^{1-q} - 1}{1-q} \right]. \tag{31}$$

Moreover, because Eq. (8) is rewritten as

$$Z_q(k) - 1 = n_q(k)\, Z_q(k)\,, \tag{32}$$

Eq. (31) becomes

$$S_q = \gamma\, k_B \int \frac{d^3\mathbf{k}}{(2\pi)^3} \left[\frac{(n_q(k))^q - 1}{1-q} + (Z_q(k))^{1-q}\, \frac{1 - n_q(k)}{1-q} \right]. \tag{33}$$

Finally, using $Z_q(k) = [\,1 - n_q(k)\,]^{-1}$ from Eq. (32), we have

$$\begin{aligned} S_q &= \gamma\, k_B \int \frac{d^3\mathbf{k}}{(2\pi)^3} \frac{(n_q(k))^q + (1 - n_q(k))^q - 1}{1-q}, \\ &= -\,\gamma\, k_B \int \frac{d^3\mathbf{k}}{(2\pi)^3} \left[\frac{n_q(k) - (n_q(k))^q}{1-q} + \frac{(1 - n_q(k)) - (1 - n_q(k))^q}{1-q} \right], \\ &= -\,\gamma\, k_B \int \frac{d^3\mathbf{k}}{(2\pi)^3} \left[(n_q(k))^q \ln_q(n_q(k)) + (1 - n_q(k))^q \ln_q(1 - n_q(k)) \right]. \end{aligned} \tag{34}$$

The result is a q-deformed extension of the Boltzmann-Fermi-Dirac entropy. The essentially same result is also derived in Ref. [17].

References

[1] C. Tsallis, Braz. J. Phys. **29** (1999) 1.

[2] Europhysics News **36** (2005) No.6 [http://www.europhysicsnews.com].

[3] C. Tsallis, http://tsallis.cat.cbpf.br/TEMUCO3.pdf.

[4] G. Wilk and Z. Włodarczyk, Phys. Rev. Lett. **84** (2000) 2770 [arXiv:hep-ph/9908459].

[5] D.B. Walton and J. Rafelski, Phys. Rev. Lett. **84** (2000) 31 [arXiv:hep-ph/9907273].

[6] K.K. Gudima, A.S. Parvan, M. Płoszajczak and V.D. Toneev, Phys. Rev. Lett. **84** (2000) 4691 [arXiv:nucl-th/0003025].

[7] C.E. Aguiar and T. Kodama, Physica A **320** (2003) 371.

[8] B.D. Serot and J.D. Walecka, *Advances in Nuclear Physics*, Vol. **16** (Plenum, New York, 1986).

[9] A. Drago, A. Lavagno and P. Quarati, Physica A **344** (2004) 472 [arXiv:nucl-th/0312108].

[10] F.I.M. Pereira, R. Silva and J.S. Alcaniz, Phys. Rev. C **76** (2007) 015201 [arXiv:nucl-th/0705.0300].

[11] K. Miyazaki, Mathematical Physics Preprint Archive (mp_arc) 06-336.

[12] S. Abe, S. Martínez, F. Pennini and A. Plastino, Phys. Lett. A **281** (2001) 126 [arXiv:cond-mat/0011012].

[13] E. Vives and A. Planes, Phys. Rev. Lett. **88** (2002) 020601 [arXiv:cond-mat/0106428].

[14] R. Toral, Physica A **317** (2003) 209.

[15] H.H. Aragão-Rêgo, D.J. Soares, L.S. Lucene, L.R. da Silva, E.K. Lenzi and Kwok Sau Fa, Physica A **317** (2003) 199.

[16] U. Tırnaklı, F. Büyükkılıç and D. Demirhan, Phys. Lett. A **245** (1998) 62 [arXiv:cond-mat/9809126].

[17] A.M. Teweldeberhan, A.R. Plastino and H.G. Miller, Phys. Lett. A **343** (2005) 71. [arXiv:cond-mat/0504516].

[18] A.S. Parvan, Phys. Lett. A **350** (2006) 331 [arXiv:cond-mat/0506392].

[19] K. Miyazaki, Mathematical Physics Preprint Archive (mp_arc) 07-64.

[20] J.B. Natowitz *et al.*, Phys. Rev. Lett. **89** (2002) 212701 [arXiv:nucl-ex/0204015].

[21] J.B. Natowitz *et al.*, arXiv:nucl-ex/0206010.

[22] S. Abe and A.K. Rajagopal, Phys. Rev. Lett. **91** (2003) 120601 [arXiv:cond-mat/0304066].

[23] J.B. Natowitz *et al.*, Phys. Rev. C **65** (2002) 034618 [arXiv:nucl-ex/0106016].

[24] K. Miyazaki, Mathematical Physics Preprint Archive (mp_arc) 07-92.

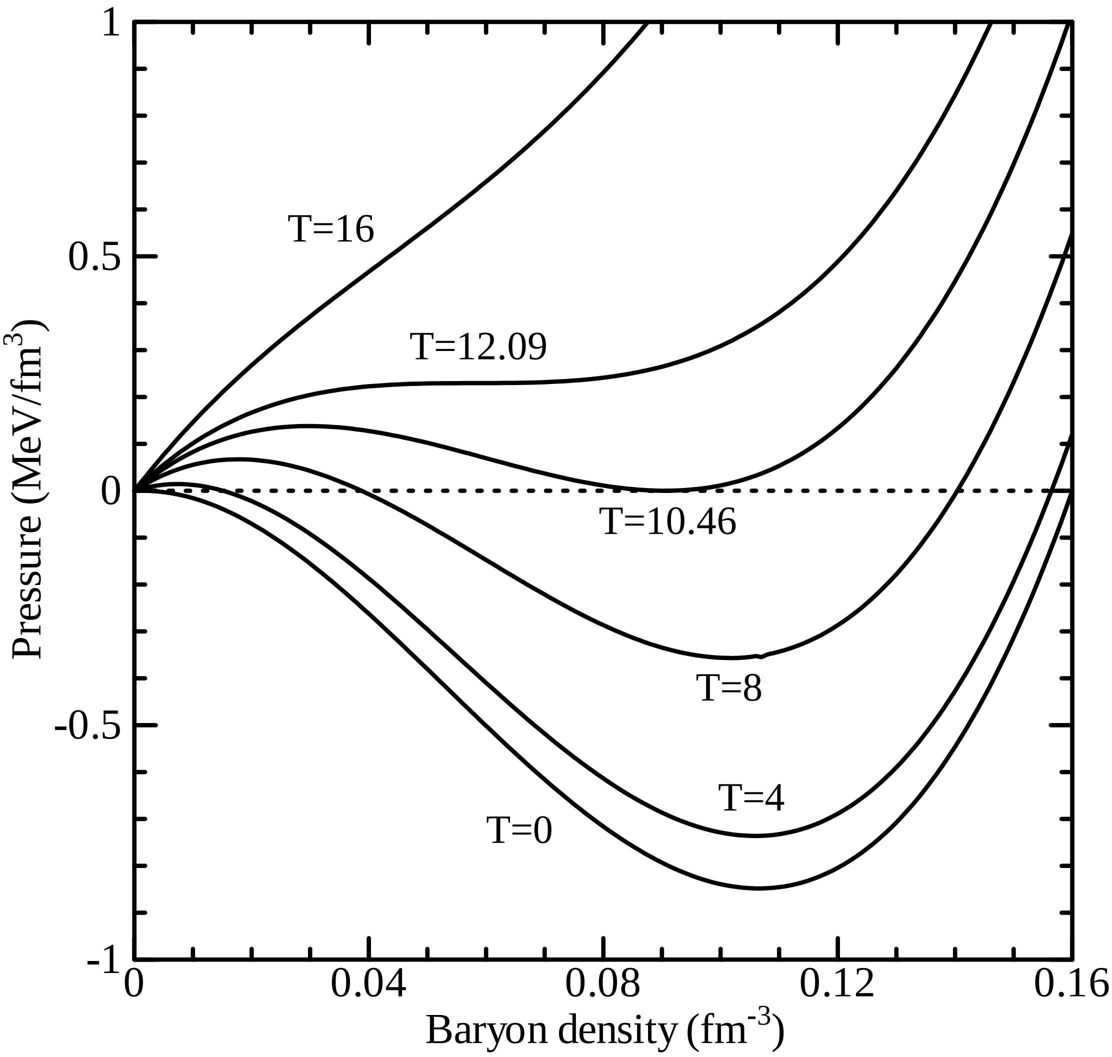

Figure 1: The isotherms of pressure-density plane for symmetric nuclear matter in the generalized thermo-statistics.

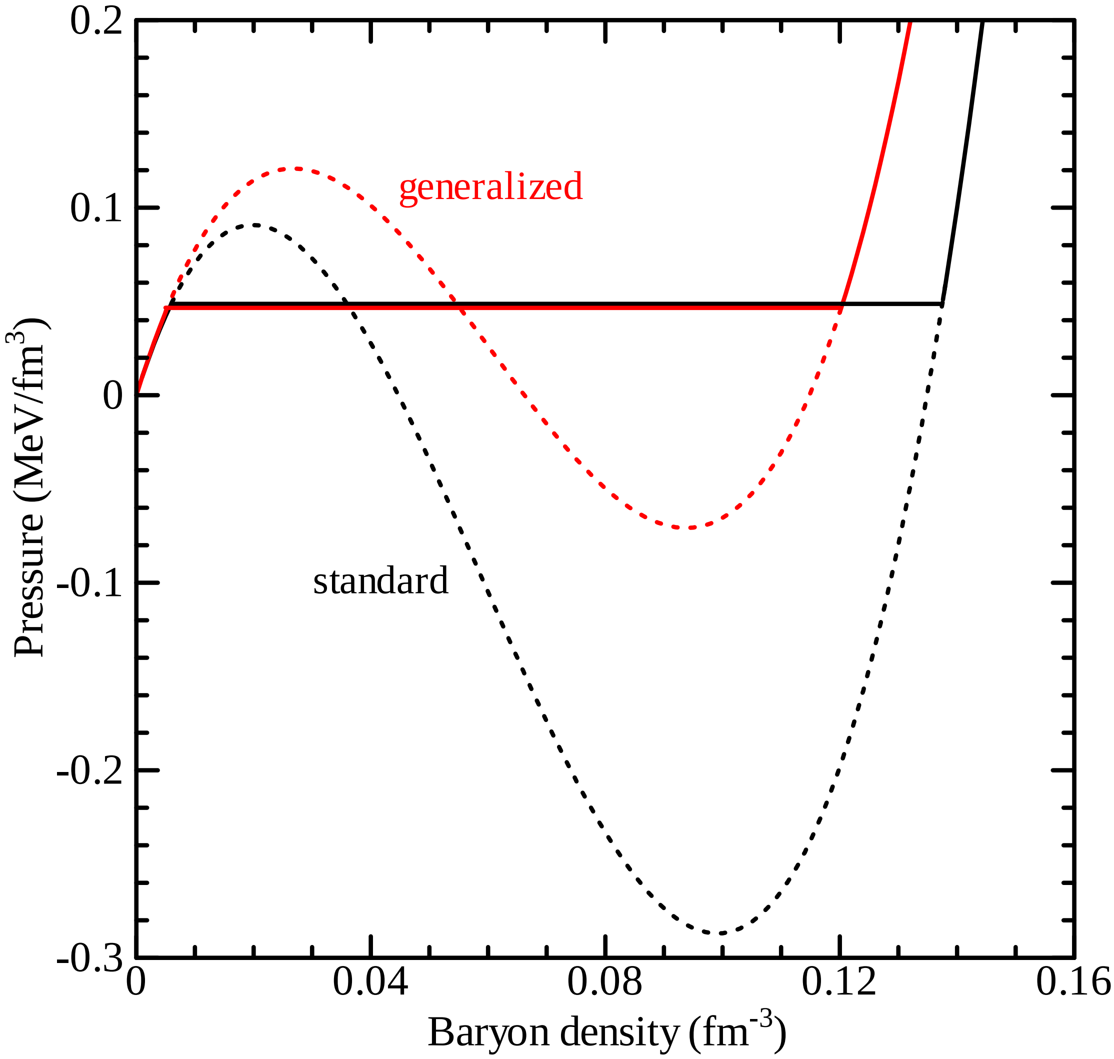

Figure 2: The black and red curves are the pressure-density isotherms at $T = 10\text{MeV}$ in the standard and generalized thermo-statistics, respectively. The horizontal lines are the equilibrium pressures of liquid-gas mixed phases from the Maxwell construction.

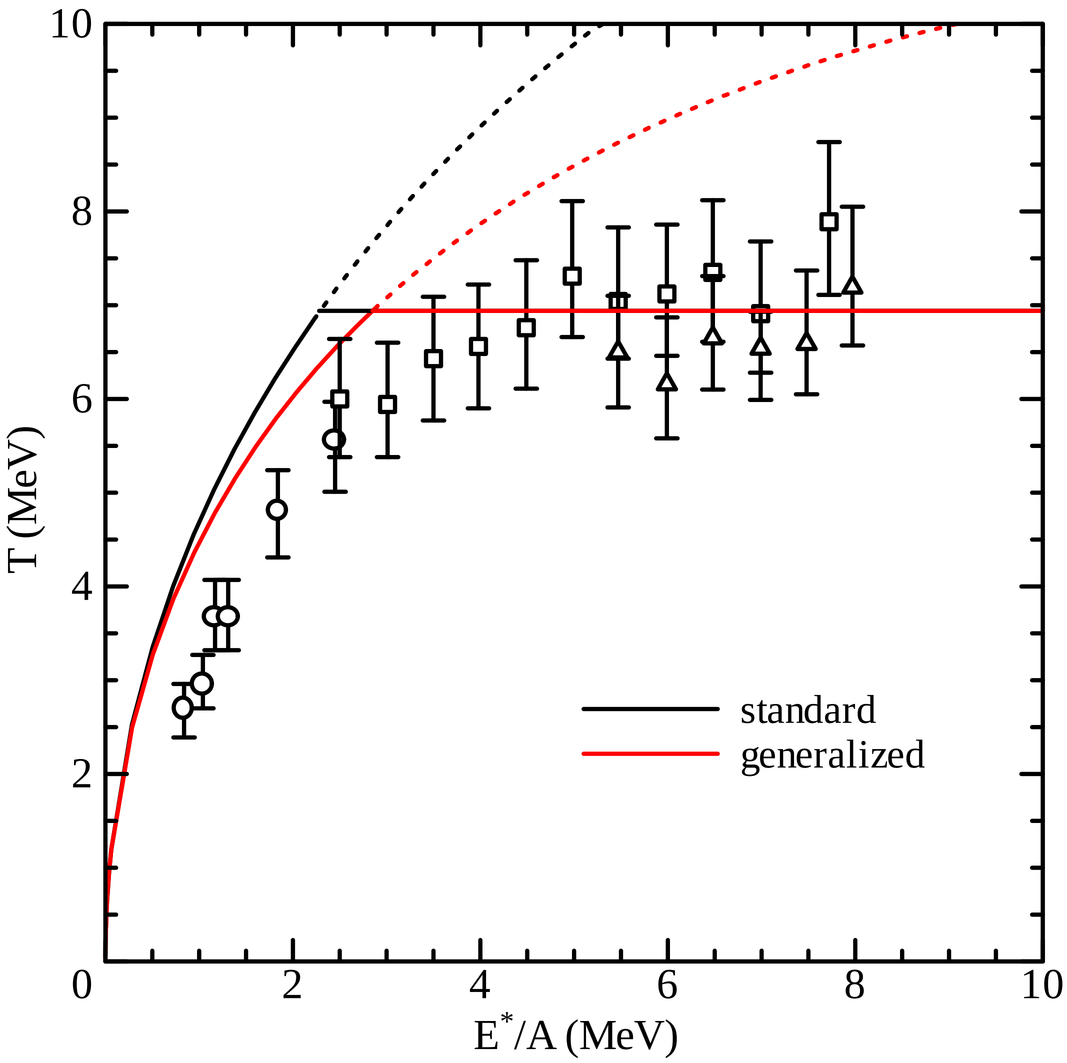

Figure 3: The black and red curves are the caloric curves of nuclear matter at $P = 0.01\text{MeV}/\text{fm}^3$ in the standard and generalized thermo-statistics, respectively. The horizontal lines are the boiling temperatures from the Maxwell construction of liquid-gas phase equilibrium. The experimental data are from Ref. [23].

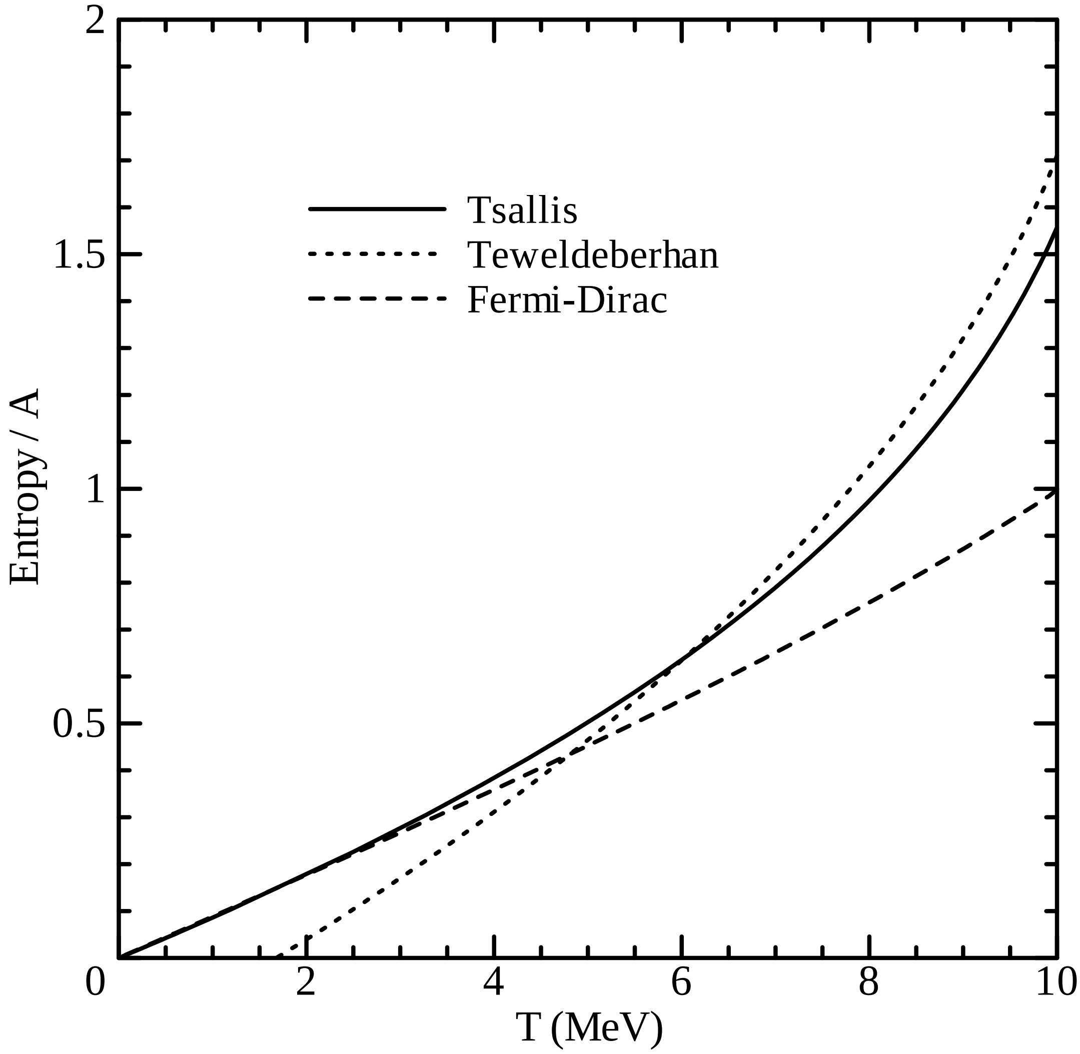

Figure 4: The Clausius entropy per baryon versus physical temperature under constant pressure $P = 0.01\text{MeV}/\text{fm}^3$. The solid and dotted curves are the results using the cut-off prescription (28) and (29), respectively. The dashed curve is the result in the standard Fermi-Dirac thermo-statistics.